

Biologically relevant *O,S*-donor compounds. Synthesis, molybdenum complexation and xanthine oxidase inhibition†‡

Sílvia Chaves,^a Marco Gil,^a Sónia Canário,^a Ratomir Jelic,^b Maria João Romão,^c José Trincão,^c Eberhardt Herdtweck,^d Joana Sousa,^e Carmen Diniz,^e Paula Fresco^e and M. Amélia Santos^{*a}

Received 8th November 2007, Accepted 10th January 2008

First published as an Advance Article on the web 20th February 2008

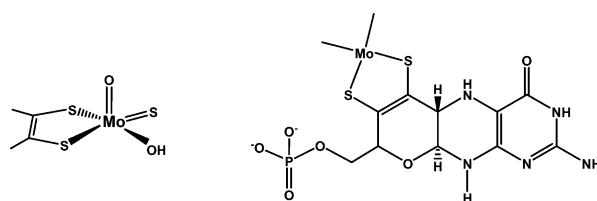
DOI: 10.1039/b717172b

Two *O,S*-donor ligands, hydroxythiopyrone and hydroxythiopyridinone derivatives, were developed and studied, as well as the corresponding *O,O*-derivatives, with a view to their potential pharmacological applications as xanthine oxidase (XO) inhibitors. The biological assays revealed that the *O,S*-ligands present high inhibitory activity towards XO (nanomolar order, close to that of the pharmaceutical drug allopurinol), in contrast to the corresponding *O,O*-analogues. Due to the biomedical relevance of this molybdenum-containing enzyme, the corresponding Mo(VI) complexes were studied both in solution and in the solid state, aimed at identifying the source of the biological properties. The solution studies showed that, in comparison with the *O,O*-analogues, the Mo(VI) complexes with the *O,S*-ligands present some stabilization, which is even more pronounced for the reduced Mo(IV) species. The crystal structures of the Mo(VI) complexes with the hydroxythiopyrone revealed good flexibility of the coordination modes, with two structural isomers and two polymorphic forms for a mononuclear and a binuclear species, respectively. These results give some support to mechanistic proposals for the XO inhibition involving the interaction of the thione group with the molybdenum cofactor, thus indicating a role of the sulfur atom in the XO inhibition.

Introduction

Molybdenum is an essential trace element, which plays an important role in many biological systems.¹ It is required as the cofactor component of various redox enzymes involved in almost all forms of life, for example, nitrate reductase in plants (crucial in the metabolism of nitrogen) and the xanthine oxidase (XO) family in humans, which is implicated in several diseases, such as gout (hyperuricemia) and cardiovascular diseases.^{2–4} Clinical and basic experiments have indicated that disorder of the XO activity is one of the principal causes of myocardial ischemic reperfusion injury and it is involved in the pathogenesis of vascular endothelial

dysfunction, hypertension and heart failure;⁵ XO catalyses the oxidative hydroxylation of purine substrates, at the molybdenum centre of the pterin cofactor, with the molybdenum coordinated to the *cis*-dithiolene group of one pyranopterin plus additional oxo, sulfido and hydroxo groups (see Scheme 1).^{2,4,6} That oxidative process generates reactive oxygen species (ROS), which can cause cell membrane disintegration, membrane protein damage and DNA mutation, initiating or propagating the development of diseases such as liver injury and cancer.



Scheme 1 Schematic representation of the Mo active site and the pyranopterin (molybdopterin) cofactor of xanthine oxidase.

Inhibition of XO activity has been recognized to improve the above pathophysiological conditions and to reduce ROS,^{7–9} thus contributing to an important chemoprevention mechanism.¹⁰

Over the past years, there has been considerable effort in the development of XO inhibitors,¹¹ especially since allopurinol was introduced in the clinical treatment of gout¹² and was also shown to decrease the extent of deleterious effects of tissue injury following ischemia reperfusion. However, adverse effects associated with the use of allopurinol prompted the need for new XO inhibitors with increased therapeutic activity and fewer or no side effects. Most of the reported potential XO inhibitors have been focused on exploitation of the organic part of the compounds in order to

^aCentro de Química Estrutural, Complexo I, Instituto Superior Técnico, Av. Rovisco Pais, 1049-001, Lisboa, Portugal. E-mail: masantos@ist.utl.pt; Fax: +351-21-8464455; Tel: +351-21-8419273

^bFaculty of Science, Institute of Chemistry, P.O. Box 60, 34000 Kragujevac, Serbia

^cREQUIMTE-CQFB, Departamento de Química, Faculdade de Ciências e Tecnologia, Universidade Nova de Lisboa, Portugal

^dTechnische Universität München, Lehrstuhl für Anorganische Chemie, Lichtenbergstrasse 4, D-85747, Garching, Germany

^eLaboratório de Farmacologia, REQUIMTE-FARMA, Faculdade de Farmácia, Universidade do Porto, Rua Anibal Cunha, 164, 4050-123, Porto, Portugal

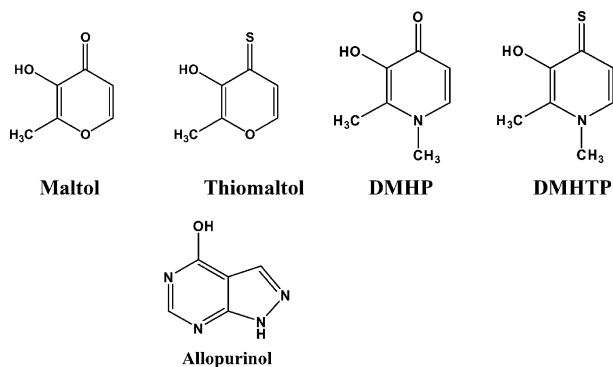
† CCDC reference numbers 664272, 656368 and 656367 for complexes α -1, β -1, and **2**. For crystallographic data in CIF or other electronic format see DOI: 10.1039/b717172b

‡ Electronic supplementary information (ESI) available: Table S1, containing global formation constants for the hydrolytic species formed in the H^+ - MoO_4^{2-} system; Fig. S2 showing a cyclic voltammogram of $MoO_2(thiomaltol)_2$; Tables S3–S8, including more detailed data of compound α -1; Fig. S9 illustrating compound α -1; Tables S10–S15 with detailed data of compound β -1; Fig. S16 showing compound β -1. See DOI: 10.1039/b717172b

improve the binding interaction with the pterin molecule and they mostly incorporate phenolic derivatives.¹³

On the other hand, complexes of molybdenum with model molecules have also become interest because of their potential application as orally active drugs for the treatment of cardiac dysfunctions associated with diabetes.^{14,15} Complexation of molybdenum(VI) with several type of *O,O*-donor ligands has been extensively studied, namely with siderophore analogues of hydroxamate or catecholate type.^{16,17} 3-Hydroxy-4-pyrones and 3-hydroxy-4-pyridinones (3,4-HP), in particular 3-hydroxy-2-methyl-4-pyrone (maltol) and 3-hydroxy-2-methyl-4-pyridinone (DMHP or DFP), are important bioligands in chelating therapy for the removal of excessive metal ions from the body, such as iron (in transfusional hemosiderosis of thalassemia major patients)^{18,19} or aluminium (due to external injuries).^{20,21} Their Mo(VI) complexes have been recently studied both in the solid state¹⁵ and in aqueous solution,²² aiming at their potential pharmacological application. Concerning the corresponding thione ligands, possessing mixed *O,S*-donor atoms, the study of their interaction with molybdenum(VI) seems also of high biological interest, either as models or as inhibitors of pterin-dependent molybdenum enzymes, the co-factors of which have the molybdenum coordinated to *S*- and *O*-donor atoms (see Scheme 1). However, unlike the study of molybdenum complexation with *O,O*-donor ligands, identical studies with *O,S*- or *S,S*-donor ligands are very scarce and mostly involve modelling the reductive half reaction occurring at the molybdenum centre of the enzymes.^{23,24}

Following our recent interest in the development of *O,O*- and *O,S*-donor ligands of 3,4-HP for Mo(VI) complexation^{22,25} and the recognized biological interest of the *O,S*-donor ligands, namely in relation to the inhibition of molybdenum-containing enzymes, we report herein the preparation of simple *O,S*-donor ligands (hydroxypyridinethione (3,4-HTP) and hydroxythiopyrone), the physicochemical properties of their Mo complexes and results of bioassays of these ligands as inhibitors of xanthine oxidase, in comparison with the *O,O*-analogues (see Scheme 2). In particular, the molybdenum complexes were investigated in solution, by UV-Vis spectrophotometry and cyclic voltammetry, and also in the solid state, by X-ray diffraction, aimed at the rationalization of the inhibition of XO activity demonstrated by the new *O,S*-compounds and also to gain some insight into potential mechanisms.



Scheme 2 Structural formulae of the synthesized compounds and allopurinol.

Results and discussion

Synthesis of the compounds

The synthesis of the *O,S*-ligands, 3-hydroxy-1,2-dimethylpyridin-4(1*H*)-thione (DMHTP) and 3-hydroxy-2-methyl-4*H*-pyran-4-thione (thiomaltol), involved the thionation of the corresponding commercially available *O,O*-derivatives, 1,2-dimethyl-3-hydroxypyridin-4(1*H*)-one (DMHP) and 3-hydroxy-2-methyl-4*H*-pyran-4-one (maltol), by refluxing with Lawesson's reagent in dry toluene, following a similar procedure to that previously reported for the preparation of thiohydroxamic acids.^{25,26} The molybdenum complexes in the solid state were readily prepared by direct addition of an ammonium molybdate aqueous solution to the thiomaltol ethanolic solution. Recrystallization from acetone and slow evaporation of this solvent led to the appearance of two different types of complexes at subsequent stages of the solvent evaporation, firstly complex **1** and then complex **2**.

Acid–base properties

For the equilibrium solution studies, spectrophotometric methods were adopted because, under the usual potentiometric concentration conditions (mM), precipitation occurred in the Mo(VI) complexation studies. The protonation constants of maltol, thiomaltol, DMHP and DMHTP were determined from spectrophotometric titrations in 15% (v/v) MeOH aqueous solutions (see Fig. 1a and 2a), at 25 °C and 0.1 M KCl, except for DMHTP, for which log K_2 (< 2) was determined by ¹H NMR titration.

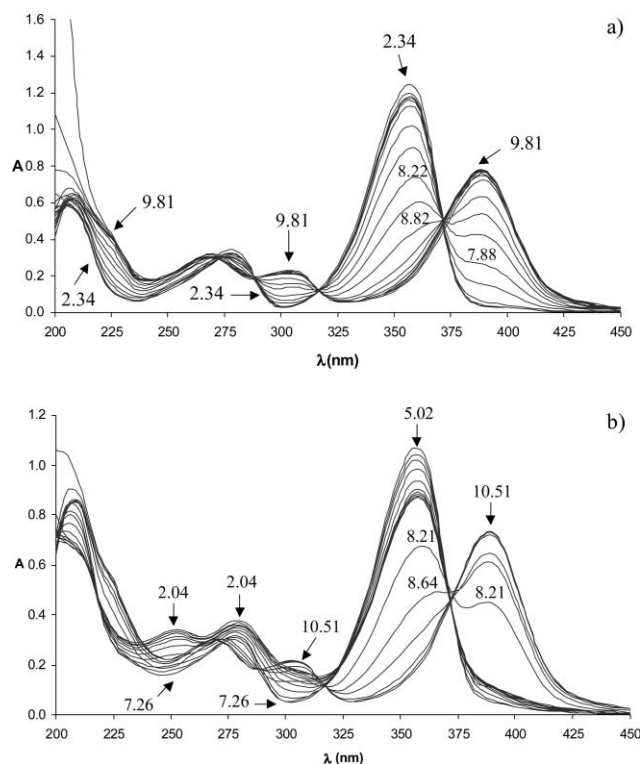


Fig. 1 Spectrophotometric absorbance curves at indicated pH values for (a) thiomaltol; (b) Mo(VI)/thiomaltol ($C_M = 2.52 \times 10^{-5}$ M, $C_L/C_M = 2$).

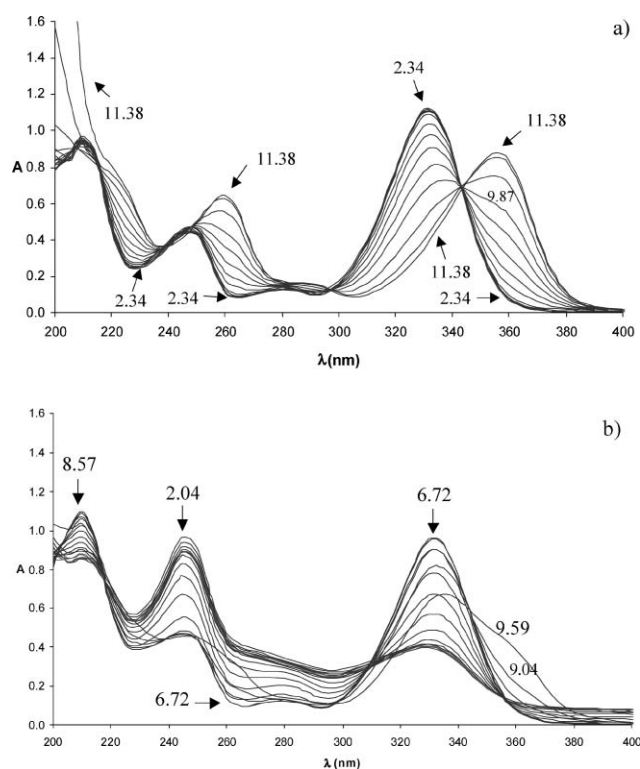


Fig. 2 Spectrophotometric absorbance curves at indicated pH values for (a) DMHTP; (b) Mo(VI)/DMHTP ($C_M = 2.52 \times 10^{-5}$ M, $C_L/C_M = 2$).

Table 1 Stepwise protonation constants ($\log K_i$) for the ligands (maltol, thiomaltol, DMHP and DMHTP) and also global formation constants and pM values of their Mo(VI) complexes ($I = 0.1$ M KCl, 15% (v/v) $\text{CH}_3\text{OH}-\text{H}_2\text{O}$, $T = 25.0 \pm 0.1$ °C)

	Maltol	Thiomaltol	DMHP	DMHTP
$\log K_1$	8.67(3) 8.67(3) ^a	8.27(1) 8.16(2) ^c	9.82(1) 9.76 ^e	9.70(1) 9.47 ^c
$\log K_2$	8.513 ^b	8.12(2) ^d	9.749(4) ^f 3.74(2) 3.62 ^e 3.655(7) ^f	9.44(1) ^d 0.95(3) ^g
$\log \beta_{\text{MoO}_2\text{L}_2}$	38.51(5)	38.50(3)	39.31(4) 40.22(4) ^f	41.48(6)
$\log \beta_{\text{MoO}_3\text{L}}$	20.71(6)	21.19(3)	20.10(4) 20.0(1) ^f	21.82(5)
pMo ^h	6.15	6.57	6.00	6.18

^a Ref. 27 ($I = 0.16$ M NaCl, $T = 37$ °C, in water). ^b Ref. 28. ^c Ref. 29 ($I = 0.10$ M KCl, $T = 25.0$ °C, in water). ^d Ref. 30 ($I = 0.16$ M NaCl, $T = 25.0$ °C, in water). ^e Ref. 31 ($I = 0.1$ M KCl, $T = 25.0$ °C, in water). ^f Ref. 22 ($I = 0.2$ M KCl, $T = 25.0$ °C, in water). ^g Determined by ¹H NMR titration. ^h pMo values ($C_{\text{Mo}} = 10^{-6}$ M, $C_L = 10^{-5}$ M, pH = 7.4).

The calculated stepwise protonation constants obtained are collected in Table 1, together with some literature values obtained under different experimental conditions.^{22,27–31}

Analysis of Table 1 shows that the fully protonated forms of these compounds have one (maltol and thiomaltol) or two (DMHP and DMHTP) dissociable protons, and the corresponding protonation constants are in agreement with values typically attributed to the corresponding hydroxyl and *N*-pyridinyl groups.³² DMHTP and thiomaltol present $\log K_1$ values (9.70 and 8.27) which

are slightly lower than those of their oxo analogues, DMHP and maltol (9.82 and 8.67), which may be attributed to the stabilisation enhancement of the corresponding conjugate bases, due to the lower electronegativity and higher polarizability of the sulfur atom, allowing greater delocalisation of the negative charge of the phenolate. There is also a decrease in H-bond interaction between the (thio)carbonyl group and the phenolic proton, as compared with the corresponding oxo compound, with concomitant decrease of the stability of the protonated species. Identical reasons explain the fact that $\log K_2$ is lower for DMHTP than DMHP. Furthermore, the higher acidity of the pyrone (or thiopyrone) hydroxyl groups, as compared to that of the corresponding pyridinone (or pyridinethione) derivatives is attributed to the higher electronegativity of the ring *O*-atom as compared to that of the *N*-CH₃ group, allowing greater stabilization of the phenolate negative charge. According to the calculated protonation constants of the compounds, the neutral HL species are predominant at physiological pH, a relevant feature for the membrane crossing ability.

Mo(VI) complexation

Solution equilibrium studies. For the study of the Mo(VI) complexes, spectrophotometric titrations were performed to avoid the precipitation problems of potentiometric titrations, because then much lower analytical concentration can be used (*ca.* 10^{-5} M). Nevertheless, in aqueous Mo(VI) systems, the free metal ion does not exist (but several hydrolytic species do) and thus MoO_4^{2-} was chosen as the metal (M) component in the calculations. Therefore, the first step for the Mo(VI) complexation study was the calculation of the overall stability constants for the Mo(VI) hydrolytic species by spectrophotometric titration, under the experimental conditions ($I = 0.1$ M KCl, 15% (v/v) $\text{CH}_3\text{OH}-\text{H}_2\text{O}$, $T = 25.0 \pm 0.1$ °C). The calculated values are summarized in Table S1 of ESI,[†] which also includes previously reported values obtained under different working conditions. These hydrolytic species absorb in the 200–250 nm range and were included in the equilibrium models of the various Mo(VI)–ligand systems. The spectral parameters of the different ligand species obtained from the acid–base studies were also introduced into the computer program to aid the fitting of the experimental data with a complexation model. Spectra for each metal–ligand systems were recorded at various pH values and the corresponding data for the Mo(VI)–thiomaltol and Mo(VI)–DMHTP systems are represented in Fig. 1b and 2b.

Comparison of Fig. 1b and 2b with Fig. 1a and 2a, respectively, reveals significant differences, especially for acidic pH values, due to the Mo–ligand transition bands but also to concomitant differences in the ligand spectra, namely in the UV range. The best fit of the experimental data was obtained for the equilibrium model for which global stability constants are reported in Table 1. The proposed equilibrium model includes bis- and mono-chelated complexes with the formation reactions represented by eqn (1) and eqn (2):



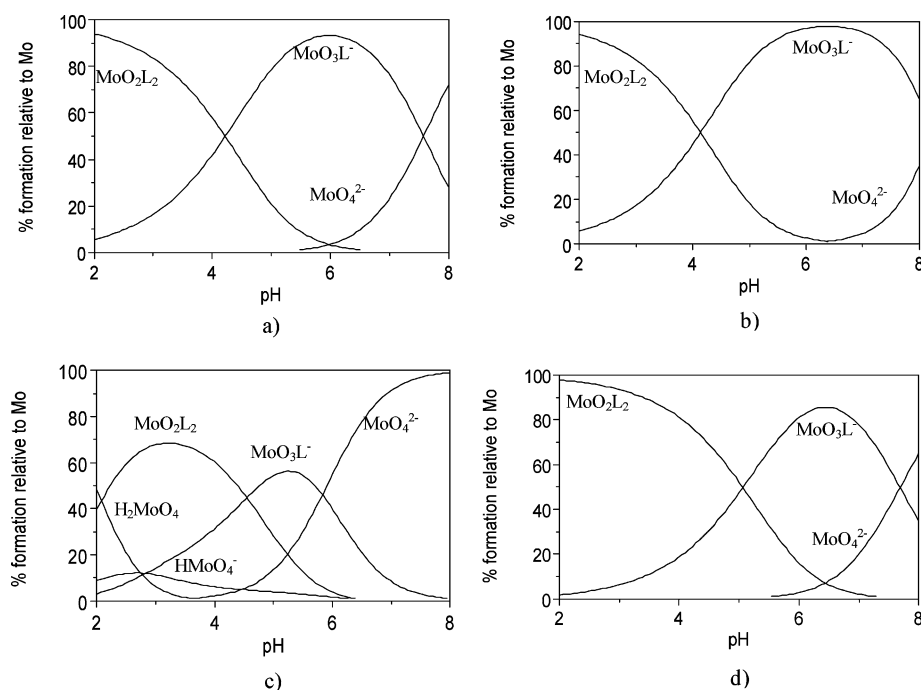


Fig. 3 Species distribution diagrams for the Mo(VI) systems with (a) maltol; (b) thiomaltol; (c) DMHP; (d) DMHTP ($C_M = 2.52 \times 10^{-5}$ M, $C_L/C_M = 2$).

pMo values (at physiological pH 7.4, $C_L/C_{Mo} = 10$, $C_{Mo} = 10^{-6}$ M) were determined (see Table 1), on the assumption that no precipitation occurs for these concentration values and also that the equilibrium model determined in this work is valid for the imposed physiological conditions. Analysis of the calculated pMo values shows that the softer *O,S*-donor ligands (thiomaltol and DMHTP) have a slightly higher affinity for the Mo(VI) than the harder *O,O*-analogues. Moreover, the formation constants obtained for DMHP are similar to those previously determined in water.²²

The concentration distribution diagrams of the Mo complex species at a 2 : 1 ligand-to-metal ion molar concentration ratio (Fig. 3) show that, under the experimental methanol–aqueous conditions, the bis-chelated species predominate below pH 4–5; above these pH values the bis-chelate species decompose through the formation of trioxo-molybdenum mono-chelate complexes with maximum percentage formation in neutral media. Furthermore, while DMHP evidences some competition between the polyoxamolybdates and the Mo–ligand complexes till pH *ca.* 5, the other ligands do not show such a strong competition, and both thiomaltol and DMHTP retard the formation of MoO_4^{2-} to higher pH values (≥ 7) than the analogous oxo complexes.

Electrochemistry

The molybdenum centre of XO participates in catalytic reactions, undergoing an oxidation state change between Mo(VI) and Mo(IV), although Mo(V) is also believed to be involved during the course of the catalysis, at least in the oxidative regeneration of the active site.²

Aimed at providing further insight into the role of the compounds as inhibitors of XO, the electrochemical behaviour of the corresponding molybdenum complexes was studied by cyclic voltammetry (CV) at a glassy carbon electrode and in a

solution of electrolyte, KNO_3 0.1 M in 20% (v/v) DMSO. The choice for this solvent was based on insolubility problems of the reagents/products in different solvents under the CV working conditions. The voltammetric measurements were performed at pH *ca.* 4 (see cyclic voltammogram of $MoO_2(\text{thiomaltol})_2$ in Fig. S2 of ESI†) because under our working conditions (concentration and ligand-to-metal stoichiometry) species distribution simulations indicated *ca.* 90% formation of the MoO_2L_2 species for all the studied binary systems.

All the Mo complexes exhibited a two-electron irreversible reduction peak (absence of oxidation peak) at: $E = -1.08$ V, for maltol; $E = -1.04$ V for thiomaltol; $E = -1.34$ V for DMHP; $E = -1.23$ V for DMHTP. The Mo(VI/IV) redox behaviour for the Mo–DMHP complex is in agreement with the value previously reported in DMSO ($E = -1.62$ V, *vs.* the $Cp_2Fe/[Cp_2Fe]^+$ couple at $E = 0$ V).³³ A comparative analysis of these results indicates that the substitution of an *O*-donor by a *S*-donor induces a positive shift of the peak potentials, similar to what is observed in other Mo(VI/IV) chelates.^{22,34} These values reflect the fact that the reduced molybdenum(IV) complexes are more stabilized by the softer *O,S*-ligands (thiomaltol and DMHTP) than by the *O,O*-ligands (maltol and DMHP).

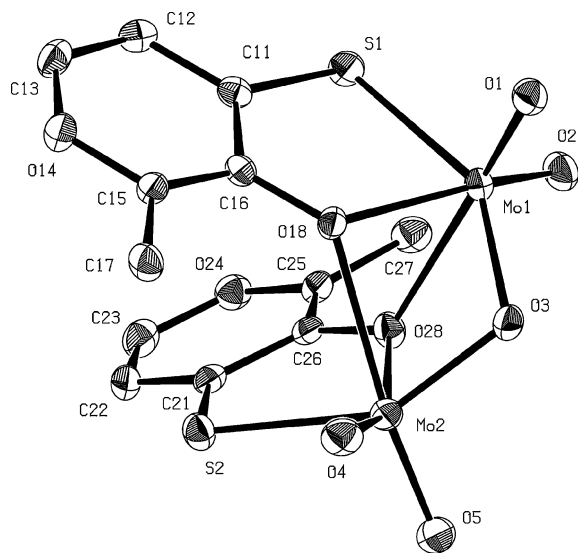
X-Ray crystallography†

Compound **1** was found in two polymorphic forms, α -**1** and β -**1**. Crystal data and data collection parameters are summarized in Table 2.

The molecular structure in the solid state of $[MoO_2(\text{thiomaltol})_2](\mu-O)$ (α -**1**), shown in Fig. 4, reveals an oxo-bridged binuclear compound. Each molybdenum atom is ligated to two terminal oxo groups, one bridging oxygen (O3) plus one sulfur and one oxygen atoms, from the thiomaltol ligand, forming a five-coordinated structure. The coordination sphere is

Table 2 Crystal data and summary of data collection and refinement of [MoO₂(thiomaltol)]₂(μ-O), complex **1**, and [MoO₂(thiomaltol)₂], complex **2**

	Complex 1		Complex 2
	α-1	β-1	
<i>Crystal data</i>			
Formula	C ₁₂ H ₁₀ Mo ₂ O ₉ S ₂	C ₁₂ H ₁₀ Mo ₂ O ₉ S ₂	C ₁₂ H ₁₀ MoO ₆ S ₂ ·1/2H ₂ O
Formula weight	554.22	554.22	419.27
Crystal system	Monoclinic	Monoclinic	Triclinic
Space group	C2/c (no. 15)	P2 ₁ /n (no. 14)	P $\bar{1}$ (no. 2)
Unit cell parameters	<i>a</i> = 31.3625(3)/Å <i>b</i> = 8.8600(1)/Å <i>c</i> = 12.3099(1)/Å β = 108.7833(6)°	<i>a</i> = 8.2509(1)/Å <i>b</i> = 13.9940(2)/Å <i>c</i> = 14.6426(2)/Å β = 105.8518(6)°	<i>a</i> = 9.8133(2)/Å <i>b</i> = 10.9684(2)/Å <i>c</i> = 14.5117(3)/Å α = 103.873(1)° β = 106.201(1)° γ = 90.026(1)°
<i>V</i> /Å ³	3238.40(6)	1626.39(4)	1452.40(5)
<i>Z</i>	8	4	4
<i>D</i> (calc.)/g cm ⁻³	2.273	2.263	1.917
μ (MoK α)/mm ⁻¹	1.853	1.845	1.217
<i>F</i> (000)	2160	1080	836
Crystal size/mm	0.05 × 0.13 × 0.13	0.10 × 0.15 × 0.23	0.20 × 0.20 × 0.02
Temperature/K	173	173	273
<i>Data collection and refinement</i>			
Wavelength/Å	MoK α 0.71073	MoK α 0.71073	MoK α 0.71073
	Rotating anode	Rotating anode	Sealed tube
θ min, max/°	1.4, 25.3	2.0, 25.3	1.51, 25
Number of reflections:			
Total	37862	40422	81371
Unique	2966	2963	5108
<i>R</i> _{int}	0.044	0.034	0.0564
Observed data (<i>I</i> > 2.0σ(<i>I</i>))	2682	2826	4450
No. reflections refined	2966	2963	5108
<i>R</i> 1 (<i>I</i> > 2.0σ(<i>I</i>))	0.0204	0.0164	0.0316
<i>wR</i> 2 (all data)	0.0476	0.0407	0.0837
Goof	1.06	1.14	0.956
Residual density (min, max)/e Å ⁻³	-0.42, 0.35	-0.31, 0.30	-0.904, 2.376

**Fig. 4** ORTEP plot of the molecular structure of [MoO₂(thiomaltol)]₂(μ-O) (α-1) with ellipsoids at 30% probability, at 173 K. Hydrogen atoms are omitted for clarity.

extended to six with a long-range contact to the oxygen atom of the adjacent thiomaltol ligand bound to the second molybdenum atom. The selected bond lengths and distances are summarized in Table 3 and a more complete list is available as ESI.†

The two Mo centers are essentially identical with no significant differences in the coordination geometry or in bond distances (see Table 3). Mo1 is coordinated to the two terminal oxo groups O1 and O2 (O4 and O5 for Mo2), to the bridging oxygen O3 and to O18 and S1 (O28 and S2 for Mo2) from the thiopyrone ring. Both Mo centers adopt a square-based bipyramidal geometry, with O1 and O28 (or O5 and O18 for Mo2) occupying the apical positions. This is true for both polymorphs.

A search in the Cambridge Structural Database³⁵ revealed over twenty Mo(vi) oxo-bridged dioxo compounds with a similar core geometry. The bond distances around the two Mo centers of both polymorphs from complex **1** are comparable to the values found for other oxo-bridged dinuclear Mo compounds. Very similar structures are exhibited by two dianionic thiophenolate complexes: [PPh₄]₂[Mo₂O₅(SC₆H₄O)₂] (CUSLIL)³⁶ and [NBu₄]₂[Mo₂O₅(SC₆H₄O)₂] (NIJGES),³⁷ which possess two dioxomolybdenum(vi) centers bridged by one μ₂-oxido and two μ₂-O-2-thiophenolate ligands. The long range distances for polymorph α-1, Mo1–O28, 2.50 Å, Mo2–O18, 2.52 Å (and for β-1 Mo1–O28, 2.55 Å, Mo2–O18, 2.61 Å) are comparable to the corresponding distances in those complexes: CUSLIL, 2.482 Å and NIJGES, 2.466 Å and 2.487 Å.

The molecular structure of [MoO₂(thiomaltol)₂] (complex **2**), the crystal data of which are given in Table 2, revealed that the asymmetric unit contains two independent molecules of [MoO₂(thiomaltol)₂] (C₁₂H₁₀MoO₆S₂) and one water molecule

Table 3 Selected bond distances (Å) and angles (°) for [MoO₂(thiomaltol)]₂(μ-O)

	α-1	β-1		α-1	β-1
<i>Selected bond distances/Å</i>					
Mo1–S1	2.4770(7)	2.4755(6)	Mo2–O4	1.702(2)	1.704(2)
Mo1–O1	1.699(2)	1.694(2)	Mo2–O5	1.699(2)	1.695(2)
Mo1–O2	1.701(2)	1.709(2)	Mo2–O18	2.521(2)	2.614(2)
Mo1–O3	1.911(2)	1.914(2)	Mo2–O28	2.158(2)	2.139(2)
Mo1–O18	2.155(2)	2.158(2)	S1–C11	1.711(3)	1.712(2)
Mo1–O28	2.500(2)	2.552(1)	S2–C21	1.720(3)	1.717(3)
Mo2–S2	2.4725(7)	2.4731(6)	O18–C16	1.331(3)	1.335(3)
Mo2–O3	1.912(2)	1.909(2)	O28–C26	1.337(3)	1.333(3)
<i>Selected bond angles/°</i>					
S1–Mo1–O1	100.55(7)	100.93(6)	S2–Mo2–O5	100.16(7)	102.15(6)
S1–Mo1–O2	88.65(7)	89.68(5)	S2–Mo2–O4	88.62(7)	88.49(5)
S1–Mo1–O3	146.38(5)	146.77(5)	S2–Mo2–O3	146.14(6)	145.87(5)
S1–Mo1–O18	77.52(5)	78.01(4)	S2–Mo2–O18	83.45(4)	83.18(3)
S1–Mo1–O28	83.33(5)	83.62(4)	S2–Mo2–O28	77.45(5)	77.89(4)
O1–Mo1–O2	104.36(9)	104.19(8)	O3–Mo2–O4	106.07(9)	103.41(7)
O1–Mo1–O3	104.37(8)	104.75(7)	O3–Mo2–O5	105.32(9)	105.39(7)
O1–Mo1–O18	97.99(8)	100.07(7)	O5–Mo2–O28	99.73(8)	99.86(7)
O1–Mo1–O28	169.35(7)	169.77(7)	O5–Mo2–O18	170.69(7)	168.21(7)
O2–Mo1–O3	106.34(9)	103.90(7)	O4–Mo2–O5	104.1(1)	104.73(8)
O2–Mo1–O18	155.56(8)	154.49(6)	O4–Mo2–O28	154.19(9)	153.93(7)
O2–Mo1–O28	85.55(8)	84.89(6)	O4–Mo2–O18	84.49(9)	85.79(6)
O3–Mo1–O18	76.99(7)	77.03(6)	O3–Mo2–O28	76.57(7)	77.88(6)
O3–Mo1–O28	68.49(7)	67.92(6)	O3–Mo2–O18	68.26(7)	66.30(5)
O18–Mo1–O28	73.01(6)	71.74(5)	O18–Mo1–O28	72.53(7)	70.74(5)
Mo1–O3–Mo2	110.81(8)	113.11(7)			

of crystallization, as depicted in Fig. 5. Unexpectedly, the two molecules are structural isomers of different geometry.

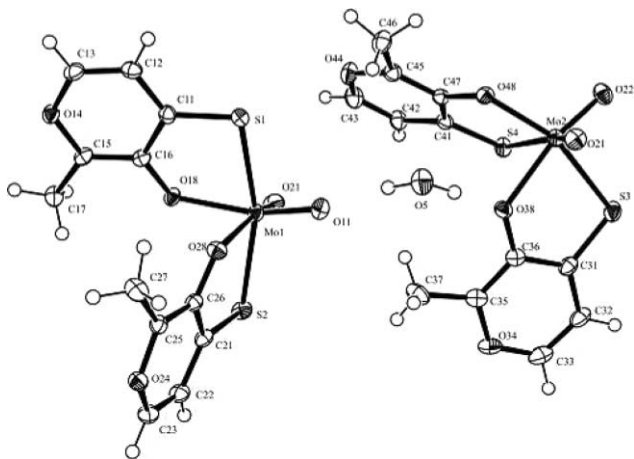


Fig. 5 ORTEP plot of the two independent structural isomers of [MoO₂(thiomaltol)]₂ in the asymmetric unit and one water molecule of crystallization, drawn with ellipsoids at 30% probability.

In both structures the Mo coordination sphere adopts a distorted octahedral geometry, in which the Mo atom is coordinated by two terminal oxo groups and two *O,S*-thiomaltol ligands. The sulfur and oxygen atoms from the thiomaltol moiety form a five-membered chelate ring with the Mo atom.

A search in the Cambridge Structural Database³⁵ revealed only five Mo(VI) dioxo compounds with two additional bidentate *O,S*-ligands and a similar core geometry (KELXII, LIMSEF, MIJCEN, MPTHMO, XAWDUV).^{37–41} With the exception of the long Mo2–S4 distance (see Table 4), all other bond distances

Table 4 Selected bond distances (Å) and angles (°) for [MoO₂(thiomaltol)]₂

Molecule A		Molecule B	
<i>Selected bond distances/Å</i>			
Mo1–O12	1.714(3)	Mo2–O21	1.708(3)
Mo1–O11	1.718(3)	Mo2–O22	1.714(3)
Mo1–O28	2.095(3)	Mo2–O48	1.975(3)
Mo1–O18	2.127(2)	Mo2–O38	2.130(2)
Mo1–S1	2.4832(10)	Mo2–S3	2.4630(10)
Mo1–S2	2.4993(10)	Mo2–S4	2.7376(9)
<i>Selected bond angles/°</i>			
O12–Mo1–O11	102.62(14)	O21–Mo2–O22	103.82(12)
O12–Mo1–O28	91.60(12)	O21–Mo2–O48	96.88(12)
O11–Mo1–O28	158.55(12)	O22–Mo2–O48	106.95(12)
O12–Mo1–O18	159.57(12)	O21–Mo2–O38	90.59(11)
O11–Mo1–O18	90.65(12)	O22–Mo2–O38	159.87(12)
O28–Mo1–O18	80.58(10)	O48–Mo2–O38	84.75(10)
O12–Mo1–S1	84.00(10)	O21–Mo2–S3	102.12(9)
O11–Mo1–S1	107.61(9)	O22–Mo2–S3	85.28(10)
O28–Mo1–S1	89.59(7)	O48–Mo2–S3	154.26(7)
O18–Mo1–S1	77.14(7)	O38–Mo2–S3	77.90(7)
O12–Mo1–S2	109.08(9)	O21–Mo2–S4	165.34(9)
O11–Mo1–S2	83.15(9)	O22–Mo2–S4	90.36(9)
O28–Mo1–S2	77.01(7)	O48–Mo2–S4	75.05(7)
O18–Mo1–S2	87.66(7)	O38–Mo2–S4	76.65(7)
S1–Mo1–S2	161.26(3)	S3–Mo2–S4	82.47(3)

around the Mo centers of both molecules A and B are comparable to values found for the related MoO₂ compounds.^{37–41}

Analysis of selected bond lengths and angles given in Table 4 (a more complete list is given in ESI†) shows that in molecule A, the two sulfur atoms are *trans* to each other, with an S1–Mo1–S2 angle of 161.26(3)°, while in molecule B they are *cis*-oriented and the corresponding angle, S3–Mo2–S4, is 82.47(3)°. This *cis* orientation of the two thiolates in molecule B has implications for the relative Mo–S distances. While the bond distance of

Mo2–S3, 2.4630(10) Å, is of the same order of magnitude as those reported for other thio complexes,^{37–42} the Mo2–S4 bond distance, 2.7376(9) Å, is significantly longer. This bond elongation can be attributed to the strong *trans* effect of a terminal oxygen *trans* to a thiolate sulfur atom, as found for Mo=O24 and Mo–S4 (O21–Mo–S4, 165.34(9)°). Similar *trans* effects of the Mo=O bond have been reported for other dioxo Mo compounds, with distances of Mo–S of 2.769 Å⁴⁰ and 2.65 Å,⁴¹ respectively. Noticeable is the fact that a similar Mo–S bond lengthening (*ca.* 0.3 Å) was also found by XAS studies on the reduced forms of xanthine oxidase and xanthine dehydrogenase,^{43,44} which was interpreted as resulting of the protonation to give a Mo^{IV}–SH group. Similar evidence for lengthening of this bond was also found in the crystal structure data of the reduced form of the aldehyde oxidoreductase.⁴⁵ However, in the present unit, excluding any H-bond interaction between that sulfur atom and the water molecule, as well as the existence of a reduced state for Mo2, the reason for the weakening of the Mo–S interaction remains unclear, although it can be probably attributed to electronic effects associated with the above-mentioned *trans* effect.

In molecule A, where the thiolate sulfurs are *cis* to the oxo groups and *trans* to each other, both Mo–S bond distances (Mo1–S1 2.4832(10) Å and Mo1–S2 2.4993(10) Å) are within the typical range for most related compounds, specifically for the XO pterin cofactor in which Mo–S (thiolate) distance is *ca.* 2.4 Å.² This is the geometry found for most related compounds.

In the asymmetric unit, one water molecule is bridging both molecules through hydrogen bonding interactions. The oxygen atom is placed at 2.797 Å (O5–O13) from the terminal oxo of molecule A and 3.011 Å (O5–O38) from the oxygen atom of one of the thiomaltol ligands of molecule B. The corresponding D–H–A angles are 170.0° and 160.9°.

The polymorphism exhibited by complex **1**, as well as the presence of the two isomers co-crystallized in complex **2**, reflect the high flexibility of both complexes, allowing changes of the coordination mode of thiomaltol.

Biological studies

Xanthine oxidase produces uric acid and superoxide and its activity has been reported to increase during oxidative stress and in radical-mediated diseases.⁴⁶ In the present work, the inhibitory activity of XO by the studied compounds was evaluated and compared with that of allopurinol. Allopurinol has a structure analogous to that of hypoxanthine and represents a competitive inhibitor of XO.⁴⁷

The compounds in this study showed an inhibitory effect on the XO-catalyzed conversion of xanthine to uric acid. It was monitored and evaluated in the presence of various concentrations of the compounds. Thiomaltol, DMHP and DMHTP were found to be good inhibitors of XO, but DMHTP was revealed to be the most promising compound, although its potency is slightly lower than that of allopurinol (see Table 5). As previously demonstrated, XO inhibitory activity can differ depending on the type of substituting groups present in the inhibitor as well as on their positions.⁴⁸ The obtained results revealed that DMHTP is a stronger XO inhibitor than DMHP, which seems to result from the presence of a sulfur donor atom in the compound backbone instead of an oxygen atom. Likewise, for the pair of

Table 5 Xanthine oxidase (XO) inhibition data of the studied compounds and of standard XO inhibitor (allopurinol), for the oxidation of xanthine to uric acid and superoxide (results are mean \pm SD (*n*))

Compound	IC ₅₀ /μM \pm SD	<i>n</i>
Maltol	1418 \pm 330	6
Thiomaltol	104 \pm 26	20
DMHP	159 \pm 52 ^a	3
DMHTP	60 \pm 35	4
Allopurinol	41 \pm 19	12

^a *p* < 0.05, from values obtained in the presence of allopurinol.

compounds maltol and thiomaltol, the sulfur compound exhibits better inhibition than the oxygen analogue. However, some sulfur compounds have been previously related with toxic properties (4-amino-6-mercaptopyrazolo[3,4-*d*]pyrimidine has toxic properties as stated in the Lancaster catalogue). This reinforces the need for more biological studies to confirm/discard any eventual toxic effect of the herein studied *O,S*-donor compounds.

Mechanistic proposals for the XO inhibition

In the present study, the inhibitory activity against XO has been found to be higher for the thio than for the oxo compounds, thus pointing towards an important role of the sulfur atom in the inhibitory cycle, probably in the reductive half-reaction of the Mo center. Moreover, as stated above, the phenolic hydroxyl groups are slightly more acidic for the studied thio compounds ($pK_a = 8.27; 9.70$) than the corresponding oxo derivatives, ($pK_a = 8.51; 9.82$) and also than the C-8 proton of xanthine ($pK_a = 14$).² Therefore, upon reduction of the Mo center, a proton can probably be transferred to the Mo=S group, followed by the nucleophilic attack of the thiolate (or phenolate) to the Mo center, while the Mo-coordinated hydroxide can exchange with the solvent. The attack of the molybdenum by the thiolate group would provide a rationale for the inhibition requirement of a thione derivative. According to this mechanistic proposal, the *O,S*-ligands (3-hydroxy-4-thiopyrone and 3-hydroxy-4-thiopyridinone) may compete with xanthine or purines, for the molybdenum center, inactivating and disabling the cofactor for the usual catalytic oxidative hydroxylation of these substrates. The formation of such a stable intermediate could be rationalized by the existence of a high affinity between the sulfur atom of the ligand and Mo(IV) (soft base and acid respectively), according to Pearson's HSAB principle,⁴⁹ as well as by the electron buffering effect of the ligand benzenoid ring. Actually, the electrochemical studies provided confirmation of the formation of stable Mo(IV) complexes with the *O,S*-ligands.

Several crystallographic studies on xanthine oxidase,^{50–52} as well as on the related enzyme (aldehyde oxido-reductase, AOR) from *Desulfovibrio gigas*,^{45,53} have led to proposals of the XO reaction mechanism. They have reported different modes of inhibition, which can be either mechanism, based on interaction of the inhibitor/substrate with the Mo of the reduced enzyme or on shape complementarities of the substrate-binding pocket.

In analogy with the XO reaction mechanism, the partial one-electron oxidation and sulfur proton dissociation may also be admitted to lead to intermediate species possessing molybdenum in the paramagnetic *v* valence state.

This work represents a first approach to the evaluation of these types of *O,S*-ligands as inhibitors of XO, but further studies will be performed to clarify the mechanism involved, including the identification of eventual Mo(v) intermediates, examination of kinetic parameters and eventual crystallographic studies of the XO–inhibitor adduct.

Experimental

General information

¹H-NMR spectra were recorded on a Varian Unity 300 MHz spectrometer at probe temperature. The following abbreviations are used: s, singlet; d, doublet. IR spectra were recorded with a Perkin-Elmer System 2000 FTIR instrument. The pD values were adjusted with DCl or CO₂ free KOD, by using a Crison 2001 instrument fitted with a combined Mettler Toledo U402-M3-S7/200 microelectrode. Melting points were determined with a Leica Galen III hot stage apparatus and are uncorrected. Elemental analyses were performed on a Fisons EA1108 CHN/F/O instrument. Mass spectra were obtained on a VG TRIO-2000 GC/MS instrument. Electronic spectra were recorded with a Perkin-Elmer Lambda 9 spectrophotometer, using 1 cm path length cells, at 25.0 ± 0.1 °C. Cyclic voltammetry was performed at room temperature using an AUTOLAB potentiostat, and a Metrohm 744 pH-meter with a Metrohm combined electrode 6.0228.000 PT1000 was used for the respective pH measurements. X-Ray diffraction studies were developed with a Nonius Kappa CCD and a Bruker X8 APEXII diffractometers. An Amplex Red Xanthine/Xanthine Oxidase Assay Kit (Invitrogen Detection Technologies, Carlsbad, CA) was used for monitoring xanthine oxidase activity and the readings were made in a BioRad Benchmark Microplate Reader (Hercules, CA).

Materials

All the chemicals were of analytical reagent grade and used as supplied without further purification. Whenever necessary, the organic solvents were purified by standard methods.⁵⁴ Where noted, compounds were purified by flash chromatography column with Merck 40–70 mesh silica gel. DMHP (1,2-dimethyl-3-hydroxypyridin-4(1*H*)-one) and maltol (3-hydroxy-2-methyl-4*H*-pyran-4-one) were purchased from Aldrich. Tetramethylsilane (TMS) and sodium 3-trimethylsilyl-*d*₄-propionate (DSS) were used as ¹H-NMR internal references in CDCl₃ and D₂O, respectively. For the electrochemical measurements the solvent was DMSO (Aldrich) and the supporting electrolyte KNO₃ (Merck).

Synthesis of ligands and molybdenum complexes

3-Hydroxy-2-methyl-4*H*-pyran-4-thione (thiomaltol). To a solution of 3-hydroxy-2-methyl-4*H*-pyran-4-one (0.40 g, 3.2 mmol) in dry toluene (25 mL), Lawesson's reagent (0.64, 1.58 mmol) was added and the mixture was left at 80 °C under nitrogen for 1 h 30 m. The reaction mixture was left to reach room temperature under nitrogen and then the solvent was removed under vacuum. The product was purified by flash chromatography, eluent CH₂Cl₂. After evaporation of the solvent, the pure product was obtained as a yellow solid. Yield: 78.3% (0.35 g); mp: 74–77 °C. IR (KBr) 1622 cm⁻¹ (ν_{C=S}). ¹H-NMR (CDCl₃/TMS): 7.77 (s, 1 H, OH), 7.59

(d, 1 H, H-Py), 7.31 (d, 1 H, H-Py), 2.45 (s, 3 H, CH₃). *m/z* (FAB): 143 (M + 1). Anal. calc. for C₆H₆O₂S: C, 50.69; H, 4.25; S, 22.55%. Found: C, 50.67; H, 4.02; S, 22.42%.

3-Hydroxy-1,2-dimethylpyridin-4(1*H*)-thione (DMHTP). To a solution of 1,2-dimethyl-3-hydroxypyridin-4(1*H*)-one (1.0 g, 7.2 mmol) in dry toluene (150 mL), Lawesson's reagent (1.45, 3.60 mmol) was added and the mixture was left refluxing under nitrogen for 4 h. The reaction mixture was left to reach room temperature under nitrogen and then the solvent was removed under vacuum. The product was purified by flash chromatography, eluent CH₂Cl₂–MeOH 12 : 1. After evaporation of the solvent, the product was obtained as a pure solid. Yield: 55% (0.61 g); mp: 165–167 °C. IR (KBr) 1622 cm⁻¹ (ν_{C=S}). ¹H-NMR (CDCl₃/TMS): 8.21 (s, 1 H, OH), 7.55 (d, 1 H, H-Py), 7.26 (d, 1 H, H-Py), 3.80 (s, 3 H, CH₃), 2.44 (s, 3 H, CH₃). *m/z* (FAB): 156 (M + 1). Anal. calc. for C₇H₉NOS: C, 54.17; H, 5.84; S, 20.66%. Found: C, 53.99; H, 5.80; S, 20.51%.

Mo–thiomaltol complex. To a solution of 3-hydroxy-2-methyl-4*H*-pyran-4-thione (30 mg, 0.21 mmol) in ethanol (2 mL), an aqueous solution (3 mL) of ammonium molybdate (0.126 g, 0.105 mmol) was added. After 2 h 30 m, the orange precipitate was filtered off and washed three times with water, ethanol and ether. The pure complex was obtained as an orange solid. Yield: 43.8% (19 mg); mp >230 °C. IR (KBr) 1572, 1497 cm⁻¹ (ν_{C=S}, ν_{C=C ring}). Anal. calc. for [MoO₂(C₁₂H₁₀O₄S₂)]: C, 35.13; H, 2.46; S, 15.63%. Found: C, 34.68; H, 2.22; S, 15.95%.

A solution of molybdenum complex (20 mg) in acetone (2 mL) was left at room temperature. Two types of yellow crystals were formed during the slow evaporation of the solvent: firstly complex **1** and then complex **2**, which were studied by X-ray diffraction.

Spectroscopic solution studies

Reagents and solutions. The molybdenum(vi) stock solution (0.1007 M) was prepared with Na₂MoO₄ and the exact metal ion concentration was determined gravimetrically *via* precipitation of the quinolin-8-olate.²² The titrant solution (0.1 M KOH) was prepared from a carbonate-free commercial concentrate (Titrisol) and standardized by potentiometric titration with potassium hydrogen phthalate; it was discarded whenever the percentage of carbonate (Gran's method)⁵⁵ was about 0.5% of the total amount of base.

Measurements. The ¹H-NMR titration of a DMHTP solution (≈0.02 M) in 15% (v/v) MeOD–D₂O with DSS was performed in NMR tubes (0.6 < pD < 7), the combined microelectrode being calibrated with standard buffered aqueous solutions. The final pD values were determined from the equation pD = pH* + 0.40,⁵⁶ in which pH* corresponds to the reading of the pH meter previously calibrated with aqueous buffers at pH 4 and 7. Spectrophotometric titrations of the ligands and their molybdenum complexes in 15% (v/v) MeOH–H₂O solution were performed at ionic strength (*I*) 0.1 M KCl. Electronic spectra were recorded in the range 200–450 nm and the working temperature was maintained at 25.0 ± 0.1 °C by using a Grant W6 thermostat. For all the samples prepared, the total volume was 20 mL, the ligand concentration was about 5.0 × 10⁻⁵ M and the Mo(vi) concentration was *ca.* 2.5 × 10⁻⁵ M. Spectrophotometric titrations of Mo(vi) solutions (C_{Mo} *ca.* 4 × 10⁻⁵ M) under the same working conditions were

also carried out to determine the Mo(VI) hydrolytic species. Under the experimental conditions used, the value determined for the ionisation constant (pK_w) was 13.84.

Calculation of equilibrium constants. The stepwise protonation constants, $K_i = [H_iL]/[H_{i-1}L][H]$, (including the log K_D value) and the overall metal-complex stability constants ($\beta_{M_mH_hL_l} = [M_mH_hL_l]/[M]^m[H]^h[L]^l$) were calculated by the fitting analysis of the spectroscopic titration data for the ligand and the ligand–Mo(VI), respectively, with the PSEQUAD program.⁵⁷ The herein determined Mo(VI) hydrolytic species were included in the equilibrium model. The species distribution curves were plotted with the HYSS program.⁵⁸

The log K_D value determined in a 15% (v/v) MeOD–D₂O solution was subsequently converted into an approximate value in H₂O by using the equation $pK_D = 0.32 + 1.044 pK_H$.⁵⁹ Although this correlation was obtained for D₂O solutions, the authors admitted that it can also give an approximate value of proton dissociation constant in the 15% (v/v) MeOD–D₂O medium.

Cyclic voltammetry measurements

Voltammetric measurements were performed in 20% (v/v) DMSO and 0.1 M KNO₃ with a three-electrode cell. A glassy carbon was used as the working electrode, a platinum electrode as auxiliary and an Ag/AgCl reference electrode. The glassy carbon electrode surface was hand polished with 0.05 μ m alumina to a mirror-like finish. In a typical experiment, the cell volume was 12 mL and the concentrations of ligand and Mo(VI) were *ca.* 6.25×10^{-4} M and 1.25×10^{-4} M, respectively. Complexes were generated *in situ* by using molybdic acid in 1 : 5 stoichiometric relation; the working pH was 4 and scans were performed at 50 mV s⁻¹. All the solutions were degassed with type U nitrogen previously bubbled through anhydrous DMSO.

X-Ray crystallographic analysis†

Crystals of [MoO₂(thiomaltol)]₂(μ -O) (compound **1**) were grown from acetone and two polymorphs were isolated: α -**1** and β -**1**. Crystals were fixed on the tip of a glass fiber and diffraction data were measured (see Table 2). The unit cell parameters were obtained by full-matrix least-squares refinement of 3170 (3102) reflections. Data collection, cell refinement and data reduction were performed using COLLECT.^{60,61} The structures were solved using SIR92⁶² and SHELXL-97,⁶³ and refined against all data. All non-hydrogen atoms were refined anisotropically. Full-matrix least-squares refinements with 266 (229) parameters were carried out by minimizing $\sum w(F_o^2 - F_c^2)^2$ with a SHELXL-97 weighting scheme. Neutral atom scattering factors for all atoms were taken from the International Tables for X-Ray Crystallography.⁶⁴

Specials for α -1: At later stages of the refinement, all hydrogen atoms could be found and were allowed to refine with individual isotropic displacement parameters. *Specials for β -1:* Methyl hydrogen atoms were calculated as a part of rigid rotating groups, with $d_{C-H} = 0.98$ Å and $U_{iso(H)} = 1.5U_{eq(C)}$. All other hydrogen atoms were placed in ideal positions and refined using a riding model, aromatic d_{C-H} distances of 0.95 Å and $U_{iso(H)} = 1.2U_{eq(C)}$. For one of the methyl groups (C17), disorder of the three hydrogen atoms could be assigned to partially occupied positions (50 : 50), which

were refined accordingly. Small extinction effects were corrected with the SHELXL-97 procedure with $\epsilon = 0.00071(11)$.

Crystals of [MoO₂(thiomaltol)]₂ (complex **2**) were grown from acetone, mounted on a glass fiber and diffraction data were measured (see Table 2). The unit cell parameters were obtained by full-matrix least-squares refinement of 9209 reflections. Data collection and cell refinement were performed with APEX2⁶⁵ and data reduction was performed with SAINT-Plus.⁶⁶ The structure was solved using the SHELXTL package,⁶⁷ and refined against all data. All non-hydrogen atoms were refined anisotropically. Full-matrix least-squares refinements with 400 parameters were carried out by minimizing $\sum w(F_o^2 - F_c^2)^2$ with a SHELXTL weighting scheme.

Biological studies

In the bioassay, xanthine oxidase catalyses the oxidation of purine bases (hypoxanthine or xanthine) to uric acid and superoxide. In the reaction mixture, the superoxide spontaneously degrades to hydrogen peroxide (H₂O₂) which, in the presence of horseradish peroxidase (HRP), reacts with Amplex Red Reagent to generate the red fluorescent oxidation product, resorufin. Resorufin has an absorption maximum of approximately 560 nm (and a fluorescence emission maximum of approximately 585 nm) and because the extinction coefficient is high (54000 cm⁻¹ M⁻¹), the assay can be performed either fluorimetrically or spectrophotometrically.

The inhibitor under study was added to the working solution containing xanthine (50 μ M), Amplex Red Reagent (0.0101 M), HRP (20 U), xanthine oxidase (XO: 1 U), and Reaction Buffer (0.125 M). Reactions were incubated at 37 °C for 30 min. Readings were made in triplicate in 96-well plates at 560 nm in a spectrophotometer. The XO inhibitory activity was expressed as the percentage of inhibition of XO, calculated as $100 - (A/B \times 100)$ where *A* and *B* are the absorbances with and without inhibitor, respectively. After fitting the data of each experiment into sigmoidal dose-response curves, IC₅₀ values were calculated and presented as mean \pm SD of *n* experiments, and compared by one-way ANOVA followed by Dunnett's *t* test. *P* values lower than 0.05 were considered to indicate statistically significant differences.

Conclusions

The set of α -hydroxythione derivatives studied in this work were revealed to be good XO inhibitors and the most promising compound (DMTHP) can be considered a potential drug candidate. The biological results have been supported not only by the solution equilibrium studies, which show that these *O,S*-compounds present a slightly higher affinity for the Mo(VI) than the corresponding *O,O*-derivatives, but also by the crystal structure results, which suggest a high flexibility for the coordination of the *O,S*-ligands to molybdenum. Moreover, the electrochemical studies also reflected the fact that the reduced Mo(IV) complexes are more stabilised by the *O,S*- than the *O,O*-ligands, which gives support to a mechanistic proposal for the XO inhibition involving the formation of a stable intermediate resulting from the attack on the molybdenum by the thiolate group. Therefore, from the physicochemical properties studied herein, it can be inferred that the sulfur atom must play an important role in the XO inhibition.

Acknowledgements

The authors thank the Portuguese Fundação para a Ciência e Tecnologia (FCT) (project PCDT/QUI/56985/04) for financial support. We also thank Dr Vitor Felix (Aveiro University) and Dr Leo Straver (Bruker-AXS BV, Delft) for help with data collection and processing of [MoO₂(thiomaltol)₂], which was measured at Bruker-AXS, Delft, The Netherlands. Dr Abhik Mukhopadhyay is also acknowledged for helpful discussions. Ratomir Jelic thanks the Ministry of Science of Serbia for financial support.

References

- 1 A. Sigel and H. Sigel, Molybdenum and Tungsten: Their Roles in Biological Processes, in *Metal Ions in Biological Systems*, Marcel Dekker, New York, 2002, vol. 39, p. 810.
- 2 R. Hille, *Chem. Rev.*, 1996, **96**, 2757–281.
- 3 Y. Yamaguchi, T. Matsumura, K. Ichida, K. Okamoto and T. Nishino, *J. Biochem.*, 2007, **141**, 513–524.
- 4 E. Garattini, R. Mendel, M. J. Romão, R. Wright and M. Terao, *Biochem. J.*, 2003, **372**, 15–32.
- 5 S. Guthikonda, C. Sinkey, T. Barenz and W. G. Haynes, *Circulation*, 2003, **107**, 416–421.
- 6 C. Brondino, M. J. Romão, I. Moura and J. J. G. Moura, *Curr. Opin. Chem. Biol.*, 2006, **10**, 109–114.
- 7 R. Butler, A. D. Morris, J. J. Belch and A. D. Struthers, *Hypertension*, 2000, **35**, 746–751.
- 8 C. E. Berry and J. M. Hare, *J. Physiol.*, 2004, **555**, 589–606.
- 9 J. Fang and M. H. Alderman, *J. Am. Med. Assoc.*, 2000, **283**, 2404–2410.
- 10 P. Fresco, F. Borges, C. Diniz and M. P. M. Marques, *Med. Res. Rev.*, 2006, **26**, 747–766.
- 11 F. Borges, E. Fernandes and F. Roleira, *Curr. Med. Chem.*, 2002, **9**, 195–217.
- 12 R. Hille and V. Massey, *Pharmacol. Ther.*, 1981, **14**, 249–26.
- 13 S. Leimkuhler, A. L. Stocker, K. Igarashi, T. Nishino and R. Hille, *J. Biol. Chem.*, 2004, **279**, 40437–40444.
- 14 A. T. Özcelikay, D. L. Becker, L. N. Ongemba, A.-M. Pottier, J.-C. Henquin and S. M. Brichard, *Am. J. Physiol. Endocrinol. Metab.*, 1996, **270**, E344–E352.
- 15 (a) S. J. Lord, N. E. Epstein, R. L. Paddock, C. M. Vogels, T. L. Hennigar, M. J. Zaworotko, N. J. Taylor, W. R. Driedzic, T. L. Broderick and S. A. Westcott, *Can. J. Chem.*, 1999, **77**, 1249–1261; (b) N. A. Epstein, J. L. Horton, C. M. Vogels, N. J. Taylor and S. A. Westcott, *Aust. J. Chem.*, 2000, **53**, 687–691.
- 16 A.-K. Duhme-Klair, G. Vollmer, C. Mars and R. Frohlich, *Angew. Chem.*, 2000, **39**, 1626–1628.
- 17 (a) E. Farkas, P. Buglyo, E. A. Enyed, V. A. Gerlei and M. A. Santos, *Inorg. Chim. Acta*, 2002, **339**, 215–223; (b) E. Farkas, H. Csóka and I. Tóth, *Dalton Trans.*, 2003, 1645–1652.
- 18 Z. D. Liu and R. C. Hider, *Med. Res. Rev.*, 2002, **22**, 26–64.
- 19 G. J. Kontoghiorghes, E. Eracleous, Ch. Economides and A. Kolganou, *Curr. Med. Chem.*, 2005, **12**, 2663–2681.
- 20 D. D. Allen, C. Orvig and R. A. Yokel, *Toxicology*, 1994, **92**, 193–202.
- 21 (a) M. A. Santos, *Coord. Chem. Rev.*, 2002, **228**, 187–203; (b) M. A. Santos, S. Gama, L. Gano and E. Farkas, *J. Inorg. Biochem.*, 2005, **99**, 1845–1852.
- 22 M. A. Santos, S. Gama, J. Costa Pessoa, M. C. Oliveira, I. Tóth and E. Farkas, *Eur. J. Inorg. Chem.*, 2007, 1728–1737.
- 23 G. M. Olson and F. A. Schultz, *Inorg. Chim. Acta*, 1994, **225**, 1–7.
- 24 P. K. Chaudhury, S. K. Das and S. Sarkar, *Biochem. J.*, 1996, **319**, 953–959.
- 25 (a) S. Chaves, M. Gil, R. Jelic and M. A. Santos, *Metal Ions in Biology and Medicine*, John Libbey Eurotext, Paris, 2006, vol. 9, pp. 13–17; (b) M. Gil, S. Chaves, R. Jelic, M. J. Romão, J. Trincão, E. Herdtweck and M. A. Santos, presented at 12th International Conference on Biological Inorganic Chemistry, 2005, Chicago, USA.
- 26 S. Prabhakar, A. M. Lobo, M. A. Santos and H. S. Rzepa, *Synthesis*, 1984, 829–830.
- 27 B. Song, N. Aebischer and C. Orvig, *Inorg. Chem.*, 2002, **41**, 1357–1364.
- 28 R. Petrola, *Finn. Chem. Lett.*, 1985, 207–212.
- 29 J. A. Lewis, B. L. Tran, D. T. Puerta, E. M. Rumberger, D. N. Hendrickson and S. M. Cohen, *Dalton Trans.*, 2005, 2588–2596.
- 30 V. Monga, B. O. Patrick and C. Orvig, *Inorg. Chem.*, 2005, **44**, 2666–2677.
- 31 R. J. Motekaitis and A. E. Martell, *Inorg. Chim. Acta*, 1991, **183**, 71–80.
- 32 M. A. Santos, M. Gil, L. Gano and S. Chaves, *J. Biol. Inorg. Chem.*, 2005, **10**, 564–580.
- 33 W. P. Griffith and S. I. Mostafa, *Polyhedron*, 1992, **11**, 2997–3005.
- 34 K. Unoura, Y. Abiko, A. Yamazaki, Y. Kato, D. C. Coomber, G. D. Fallon, K. Nakahara and A. M. Bond, *Inorg. Chim. Acta*, 2002, **333**, 41–50.
- 35 F. H. Allen and V. J. Hoy, The Cambridge Structural Database (CSD), *International Tables for Crystallography*, 2006, Vol. F, ch. 24.3, pp. 663–668.
- 36 W. Xiu-Jian, C. Zhen-Feng, L. Hong and Y. Kai-Bei, *Jiegou Huaxue*, 1997, **16**, 403–407.
- 37 C. D. Garner, J. R. Nicholson and W. Clegg, *Angew. Chem., Int. Ed. Engl.*, 1984, **23**, 972–973.
- 38 P. Palanca, T. Picher, V. Sanz, P. Gomez-Romero, E. Llopis, A. Domenech and A. Cervilla, *J. Chem. Soc., Chem. Commun.*, 1990, 531–533.
- 39 J. Li-Kao, O. Gonzalez, R. F. Baggio, M. T. Garland and D. Carrillo, *Acta Crystallogr., Sect. C: Cryst. Struct. Commun.*, 1995, **51**, 575–578.
- 40 H. Liang, Z.-F. Chen, R.-X. Hu, Q. Yu, Z.-Y. Zhou and X.-G. Zhou, *Transition Met. Chem.*, 2002, **27**, 102–104.
- 41 C. A. Cliff, G. D. Fallon, B. M. Gatehouse, K. S. Murray and P. J. Newman, *Inorg. Chem.*, 1980, **19**, 773–775.
- 42 J. M. Berg, K. O. Hodgson, S. P. Cramer, J. L. Corbin, A. Elsberry, N. Pariyadath and E. I. Stiefel, *J. Am. Chem. Soc.*, 1979, **101**, 2774–2776.
- 43 S. P. Cramer and R. Hille, *J. Am. Chem. Soc.*, 1985, **107**, 8164.
- 44 S. P. Cramer, R. Wahl and R. V. Rajagopalan, *J. Am. Chem. Soc.*, 1981, **103**, 7721–7727.
- 45 R. Huber, P. Hof, R. O. Duarter, J. J. G. Moura, I. Moura, M.-Y. Liu, J. LeGall, R. Hille, M. Archer and M. J. Romão, *Proc. Natl. Acad. Sci. U. S. A.*, 1996, **93**, 8846–8851.
- 46 W. K. Adkins and A. E. Taylor, *J. Appl. Physiol.*, 1990, **69**, 2012–2018.
- 47 H. Tamta, S. Kalra and A. K. Mukhopadhyay, *Biochemistry (Moscow)*, 2006, **71**, S49–S54.
- 48 D. E. C. Van Hoorn, R. J. Nijveldt, P. A. M. Van Leeuwen, Z. Hofman, L. M'Rabet, D. B. A. De Bont and K. Van Norren, *Eur. J. Pharmacol.*, 2002, **451**, 111–118.
- 49 R. G. Pearson, *J. Am. Chem. Soc.*, 1963, **85**, 3533–3539.
- 50 K. Okamoto, B. T. Eger, T. Nishino, S. Kondo, E. F. Pai and T. Nishino, *J. Biol. Chem.*, 2003, **278**, 1848–55.
- 51 K. Okamoto, K. Matsumoto, R. Hille, B. T. Eger, E. F. Pai and T. Nishino, *Proc. Natl. Acad. Sci. U. S. A.*, 2004, **101**, 7931–6.
- 52 J. J. Truglio, K. Theis, H. L. E. R. Silke Leimku, R. Rappa, K. V. Rajagopalan and C. Kisker, *Structure*, 2002, **10**, 115–125.
- 53 M. J. Romão, M. Archer, I. Moura, J. J. G. Moura, J. LeGall, R. Engh, M. Schneider, P. Hof and R. Huber, *Science*, 1995, **270**, 1170–1176.
- 54 *Purification of Laboratory Chemicals*, ed. W. L. F. Armarego and D. D. Perrin, Butterworth-Heinemann Press, Oxford, 1999, 4th edn.
- 55 F. J. C. Rossotti and H. Rossotti, *J. Chem. Educ.*, 1965, **42**, 375–378.
- 56 A. K. Covington, M. Paabo, R. A. Robinson and R. G. Bates, *Anal. Chem.*, 1968, **40**, 700–706.
- 57 L. Zékány and I. Nagypál, *Computational Methods for the Determination of Stability Constants*, Plenum Press, New York, 1985, pp. 291–353.
- 58 P. Gans, A. Sabatini and A. Vacca, *Talanta*, 1996, **43**, 1739–1753.
- 59 R. Delgado, J. J. R. Frausto da Silva, M. T. S. Amorim, M. F. Cabral, S. Chaves and J. Costa, *Anal. Chim. Acta*, 1991, **245**, 271–282.
- 60 R. Hooft, *COLLECT Data Collection Software for Nonius Kappa CCD*, Nonius B. V., Delft, The Netherlands, 1998.
- 61 Z. Otwinowski and W. Minor, *Methods Enzymol.*, 1997, **276**, 307–326.
- 62 SIR92: A. Altomare, M. C. Burla, M. Camalli, G. Cascarano, C. Giacovazzo, A. Guagliardi and G. Polidori, *J. Appl. Crystallogr.*, 1994, **27**, 435–441.
- 63 G. M. Sheldrick, *SHELXL-97, Program for refinement of crystal structures*, University of Göttingen, Germany, 1997.
- 64 A. J. C. Wilson, *International Tables for Crystallography*, vol. C, 3rd edn, Kluwer Academic Publishers, Dordrecht, The Netherlands, 1992.
- 65 APEX2, Version 2.1-RC13, Bruker Nonius BV, Delft, The Netherlands, 2006.
- 66 SAINT-Plus, Version 7.23a, Bruker AXS Inc., Madison, Wisconsin, USA, 2005.
- 67 SHELXTL, Version 6.12, Bruker AXS Inc., Madison, Wisconsin, USA, 2001.